Biointerphases (2012) 7:45
DOI 10.1007/s13758-012-0045-7

ARTICLE

Carbondioxide Gating in Silk Cocoon

Manas Roy · Sunil Kumar Meena · Tejas Sanjeev Kusurkar · Sushil Kumar Singh · Niroj Kumar Sethy · Kalpana Bhargava · Sabyasachi Sarkar · Mainak Das

Received: 19 April 2012 / Accepted: 26 June 2012 / Published online: 12 July 2012

Abstract Silk is the generic name given to the fibrous proteins spun by a number of arthropods. During metamorphosis, the larva of the silk producing arthropods excrete silk-fiber from its mouth and spun it around the body to form a protective structure called cocoon. An adult moth emerges out from the cocoon after the dormant phase (pupal phase) varying from 2 weeks to 9 months. It is intriguing how CO_2/O_2 and ambient temperature are regulated inside the cocoon during the development of the pupa. Here we show that the cocoon membrane is asymmetric, it allows preferential gating of CO_2 from inside to outside and it regulates a physiological temperature inside the cocoon irrespective of the surrounding environment temperature. We demonstrate that under simulating CO_2 rich external environment, the CO_2 does not diffuse inside the cocoon. Whereas, when CO_2 was injected inside the cocoon, it diffuses out in 20 s, indicating gating of CO_2 from inside to outside the membrane. Removal of the calcium oxalate hydrate crystals which are naturally present on the outer surface of the cocoon affected the complete blockade of CO_2 flow from outside to inside suggesting its role to trap most of the CO_2 as hydrogen bonded bicarbonate on the surface. The weaved silk of the cocoon worked as the second barrier to prevent residual CO_2 passage. Furthermore, we show that under two extreme natural temperature regime of 5 and 50 °C, a temperature of 25 and 34 °C respectively were maintained inside the cocoons. Our results demonstrate, how CO_2 gating and thermoregulation helps in maintaining an ambient atmosphere inside the cocoon for the growth of pupa. Such natural architectural control of gas and temperature regulation could be helpful in developing energy saving structures and gas filters.

M. Roy · S. Sarkar (✉)
Department of Chemistry, Indian Institute of Technology Kanpur, Kanpur 208016, Uttar Pradesh, India
e-mail: protozyme@gmail.com

S. K. Meena
Department of Electrical Engineering, Indian Institute of Technology Kanpur, Kanpur 208016, Uttar Pradesh, India

T. S. Kusurkar · M. Das (✉)
Department of Biological Sciences and Bioengineering, Indian Institute of Technology Kanpur, Kanpur 208016, Uttar Pradesh, India
e-mail: mainakd@iitk.ac.in

S. K. Singh
Solid State Physics Laboratory, Defense Research Development Organization, Lucknow Road, Timarpur, Delhi 110054, India

N. K. Sethy · K. Bhargava
Defense Institute of Physiology and Allied Sciences, Defense Research Development Organization, Lucknow Road, Timarpur, Delhi 110054, India

1 Introduction

Silk is the generic name given to the fibrous proteins produced by a number of arthropods. Most of these silk producing arthropods have four different stages in their life cycle. The four different stages are as follows: adult moth, eggs, larva (feeding phase) and pupa (dormant phase). An adult moth lay eggs. These eggs develop to form larva. The larval phase is the feeding phase. During this phase, the larva feeds extensively on the leaves and start excreting silk-fiber from its mouth and spun it around the body to form a protective structure called cocoon. When the larva enclosed itself inside the cocoon, it goes into the dormant phase called pupal phase. This dormant phase varies from species to species and may last from few weeks to as long

as 9 months. Once the dormant phase is over, the adult moth emerges out of the cocoon. This whole transition in the life cycle of the silk producing arthropods is termed as metamorphosis (Fig. 1). The commercial silk fiber is derived from the cocoon after removal of the pupa [1–3].

Silk fiber consists of two main proteins, fibroin and sericin. Fibroin is the structural protein and sericin is a glue like protein surrounding the fibroin protein. Silk fibers are conglutinated with a non-woven structure by sericin bonding matrix. This structural strategy must have evolved for a protective function to safe guard the development of the pupa within the silkworm cocoons, which have additional composite materials to augment the protection. Through evolutionary pressures over millions of years, cocoons have optimized their composite structure to function for the full development of silkworm pupa in the process of metamorphosis to moths. This process varied from few weeks to several months depending on the types of cocoons. During this time, cocoons are exposed to a wide range of threats such as physical attack from animals, birds or insects including bacteria. Besides, such composite structure of cocoons protect the pupa inside from harsh environmental conditions. It is of interest to understand how silk cocoon membrane performs such activity based on their porous structure, mechanical strength, and its potential for control of the gaseous environment and temperature inside. One should try to understand, how life inside a narrow confinement of cocoon breath for so many days and the most important aspect here is to address the structure of cocoons which is optimized to function in such a manner [4–18].

The cocoon offers an physically isolated space for the development of the pupa. In such an isolation, it is of paramount importance that the living species can effectively respire. To do so, the cocoon membrane should be able to flush out CO_2 from the confined chamber and allows uninterrupted inflow of fresh air. In addition to this directional flow of air and CO_2 across the cocoon membrane, effective thermoregulation is essential for its survival. Literature remain almost silent on the issue of such directional gaseous flow across the cocoon membrane [19]. Though temperature regulation studies have been attempted [9, 20, 21]. Therefore it is of great interest to understand this important feature of cocoon which impart a conducive environment for the survival of the pupa.

Here we show for the first time that the cocoon membrane is asymmetric and acts as a gas filter allowing gating (unidirectional flow) of CO_2 from inside to outside the cocoon. In contrast, the membrane promotes bidirectional flow of O_2. Further, the membrane acts as a thermo-regulator which regulates ambient temperature inside the cocoon. Bio-mimicry of such regulatory membrane using modern nano-structural materials could lead to the development of environment friendly, energy saving building materials and gas filters.

2 Materials and Methods

2.1 Procurement and Processing of the Native Cocoons

The semi-domesticated, reared variety of DABA Tasar silkworm (*Antheraea mylitta* Drury) which are reared in the state of Chhattisgarh of India was used for this study. These are naturally reared on Saja (*Terminalia tomentosa*)

Fig. 1 The metamorphosis in the life-cycle of the Tasar silkworm (*Antheraea mylitta Drury*): **a** An adult moth. **b** Eggs laid by an adult moth. **c** Fully developed pupa taken out from the cocoon. **d** Adult moth emerged out from the silk cocoon

& Arjuna (*Terminalia arjuna*) trees. Both these trees are rich source of oxalic acid and tannins. The silkworm larva fed on the leaves of these trees. Generally at the lower altitudes (50–30 m AMSL), it is reared three times a year in July–August (Rainy cocoon crop), September–October (Autumn cocoon crop) and November–December (Winter cocoon crop). We procured the cocoons from all three seasons and used them for our experiments. The procured cocoons were stored in dry cabinets. Before starting the experiments, all the cocoons were kept in a incubator (30 °C, Relative humidity 80 %) for 2 h. The pupa were removed from all the cocoons which were used for the experiments by giving a very small incision at the top.

2.2 Leaching of the Calcium Oxalate from the Outer Surface of the Cocoon

The cocoons were first treated with dilute hydrochloric acid (3 N) and after half an hour the cocoons were taken out and immersed in sodium-EDTA solution (0.4 M) stirred for 15 min and then these cocoons were taken out and washed thoroughly with plentiful of running water. These were then dried under ambient condition. These treated cocoons were subjected to microscopic analysis and gating experiments for comparison with the data obtained from native, raw cocoons. The leached out solution of cocoon has been treated to get back the calcium oxalate monohydrate which was washed out from the outer surface of the cocoons by acid treatment. It is well known that calcium oxalate can be readily solubilized in water by adding dilute hydrochloric acid, where by the oxalate ion gets protonated with the separation of oxalic acid and in forming calcium chloride. Therefore in order to recover calcium oxalate from this solution, it was first neutralized by adding ammonia solution under warm condition and this ammoniacal solution on digestion in the water bath resulted in the white precipitate of calcium oxalate monohydrate. This mixture was allowed to cool on standing and the precipitate was filtered off, washed couple of times with cold water and dried. This white residue is subjected to X-ray diffraction (XRD) and fourier transform infrared spectroscopy (FTIR) studies.

2.3 Scanning Electron Microscopy (SEM) and Energy Dispersive Spectroscopic (EDAX) Analysis

SEM analysis was done using SUPRA 40VP field emission scanning electron microscope (Carl Zeiss NTS GmbH, Oberkochen (Germany) equipped with EDAX analysis facility.

2.4 X-Ray Diffraction Studies (XRD)

XRD analysis was done using PANalytical X'Pert PRO diffractometer using CuKα radiation.

2.5 Fourier Transform Infrared Spectrometer (FTIR)

FTIR spectra of the samples were done on a Bruker fourier transform infrared spectrometer (Vector 22 model). This model works with a globar lamp source, a KBr beam splitter, and DTGS/KBr detector. The spectra were recorded in the solid state in KBr pellets. In the employed configuration, it has been possible to cover the 400–4,000 cm^{-1} range with a resolution of 4 cm^{-1}.

2.6 Studying the Flow of CO_2 Across the Cocoon Membrane

The set-up for detecting the flow of CO_2 across the cocoon membrane has been described in Fig. 2a, b.

2.7 Studying the Flow of O_2 Across the Cocoon Membrane

Figure 2c, d describes the set-up to study the flow of O_2 across the cocoon membrane.

2.8 Temperature Measurement

We cut open the cocoon at the top and removed the dead pupa and sealed the cocoon by placing a thermocouple probe (Kiethley 6517B) inside the cocoon. Before placing the cocoons in the incubator, we measured the initial temperature of the cocoons using the thermocouple probe. It is our consistent observation that the ambient temperature inside the cocoon was 2 °C more than the room temperature. All the measurements were made at a room temperature of 26 °C.

2.9 Statistical Analysis

All the statistical significance were calculated using "two-sample Students t test". The significance level was indicated by p value and significance was determined at three different p values ($p = 0.001, 0.01, 0.05$). All the results were expressed as mean ± standard error, n = number of cocoons.

3 Results and Discussion

3.1 Visual Observation

On visual observation, the outer surface of the cocoon exhibited extremely rough morphology as compared to the inner surface (Fig. 3a).

3.2 SEM Analysis of the Native Cocoon

On SEM analysis, we found the presence of large number of cuboidal shaped crystals on the outer surface of silk fibers

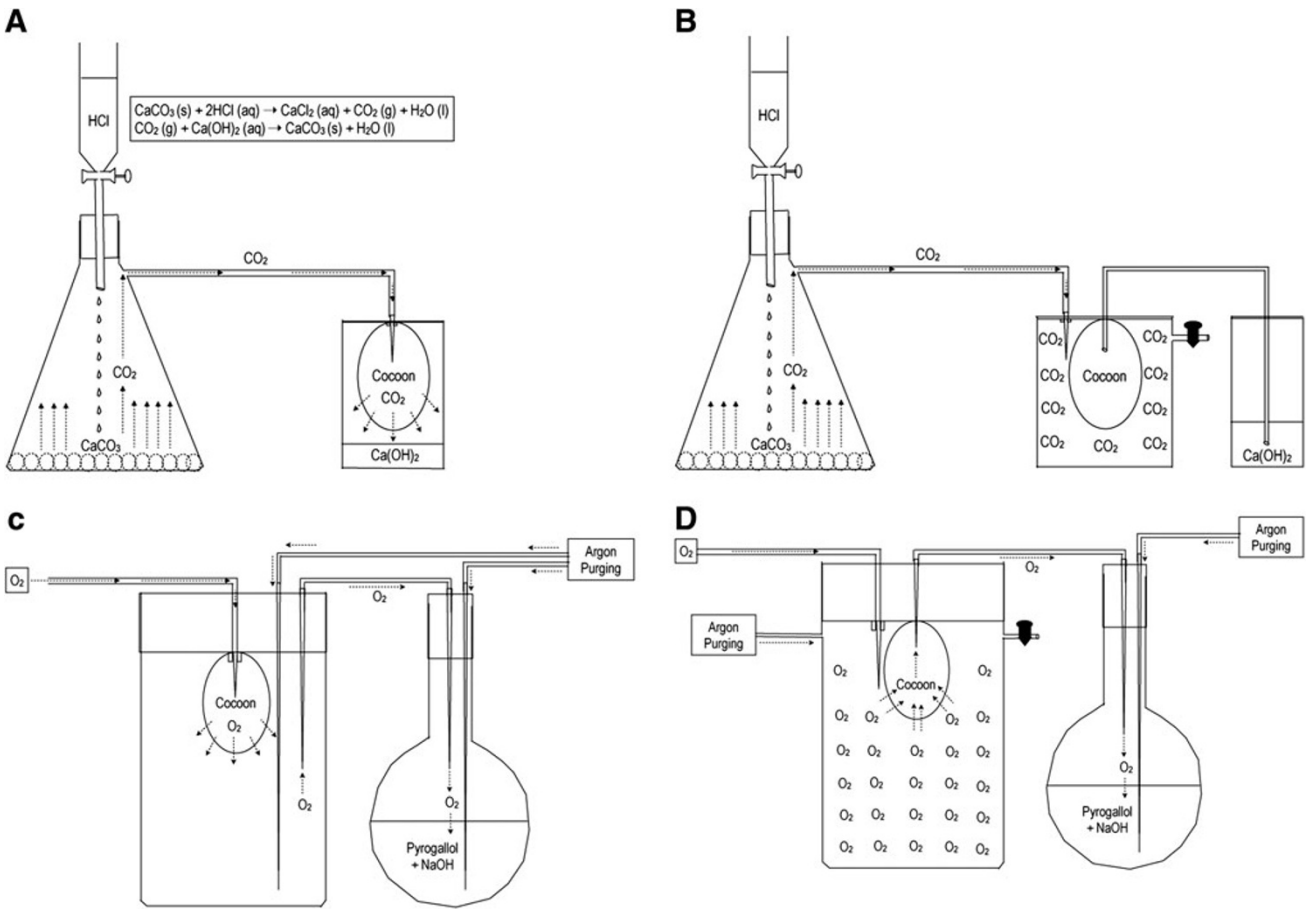

Fig. 2 **a** Schematic experimental set-up to study the diffusion of CO_2 from inside to outside the cocoon: The dead pupa was removed from the cocoon by making a narrow cut at the top of the cocoon and this cut was sealed by wrapping with a narrow band of para-film keeping the surface intact. A narrow glass tube was inserted on the top of the cocoon to supply CO_2 gas. The cocoon was allowed to hang in an air-tight beaker container containing $Ca(OH)_2$ solution. CO_2 was generated as shown in the figure using $CaCO_3$ and dilute HCl solution. As soon as CO_2 gas was allowed to pass inside the cocoon through the glass tube, the CO_2 started diffusing out of the cocoon. We recorded the time as soon as we observed the appearance of milky white smear on the $Ca(OH)_2$ solution. **b** Schematic experimental set-up to study the diffusion of CO_2 from outside to inside the cocoon: the dead pupa was removed from the cocoon and the cut was sealed by para-film. A narrow glass tube was inserted into the cocoon and the other end of the tube was immersed in $Ca(OH)_2$ solution in a beaker which was maintained under the blanket of argon flow to prevent contamination from aerial carbon dioxide. The cocoon was hung in an air tight beaker having an inlet for the passage of CO_2 with a narrow hole at a distance for free gas passage. Sometimes we blocked this narrow passage to generate CO_2 pressure on the outer surface of the cocoon. The generated CO_2 gas was allowed to pass for more than 10 min. We performed this experiment on 11 different cocoons (n = 11) and in each case the $Ca(OH)_2$ solution remained unaffected. **c** Schematic experimental set-up to study the diffusion of O_2 from inside to outside the cocoon: the experimental set-up was similar to the CO_2 detection setup. Except O_2 detection was done by using sodium pyrogallate as an absorbent. On absorbing O_2, the color of the sodium pyrogallate solution changes to dark brown. This experiment needed an extremely inert environment. Inert environment was created by purging the set-up with excess argon gas. When under argon purging the pyrogallol solution remained pale yellow, the valve of the oxygen cylinder was opened very gently and within minutes the indicator solution turned deep-brown showing the diffusion of O_2 from inside to outside of the cocoon membrane. The experiment was repeated with 10 different cocoons showing the same result. **d** Schematic experimental set-up to study the diffusion of O_2 from outside to inside the cocoon: the preparation of empty cocoon was done as described earlier. The alkaline pyrogallol solution was placed under constant argon purging to avoid interaction with air. The set up was first purged with argon for 30 min and then a flow of oxygen gas was introduced. Within minutes the pale yellow pyrogallol solution turned deep brown. The experiment was repeated with 10 different cocoons showing the same result

(Fig. 3b–d). These varied size crystals were randomly stacked over one another like tiles covering the silk thread and later identified as the crystals of calcium oxalate monohydrate by XRD and FTIR studies. In contrast, the inner surface of the cocoon was found to be extremely smooth (Fig. 3 a) with intertwined cross-network of the fibers (Fig. 3e, f). Hardly any crystals were observed on the inner surface of the cocoon.

3.3 SEM Analysis of the Cocoons After Washing Away the Calcium Oxalate Monohydrate Layer from the Outer Surface

Figure 3g, h showed the SEM images of the outer surface of the treated cocoons. On comparison with the outer surface of the untreated cocoons, it is clearly demonstrated

that the calcium oxalate monohydrate layer has completely leached away from the outer surface of the cocoon. As expected, there is hardly any noticeable change in the inner surface of the treated cocoon compared to that with the untreated cocoons (Fig. 3i).

3.4 XRD Analysis

Using XRD analysis, we found that the cuboidal crystals on the outer surface of the cocoon are of calcium oxalate monohydrate (Fig. 4). We first obtained the XRD pattern of pure calcium oxalate monohydrate. Next we obtained the XRD pattern of calcium oxalate monohydrate scrapped out from the untreated cocoon. Afterward we treated the cocoon with dilute acidified (3 N HCl) solution followed by EDTA (0.4 M) solution with the theme to leach out the calcium oxalate monohydrate from the outer surface of the cocoon. The acid washed solution in the leaching process was concentrated to reduce volume and the extra acid is being neutralized by adding ammonia wherein the leached out calcium oxalate monohydrate is re-precipitated out under warm condition for favorable granular growth. This

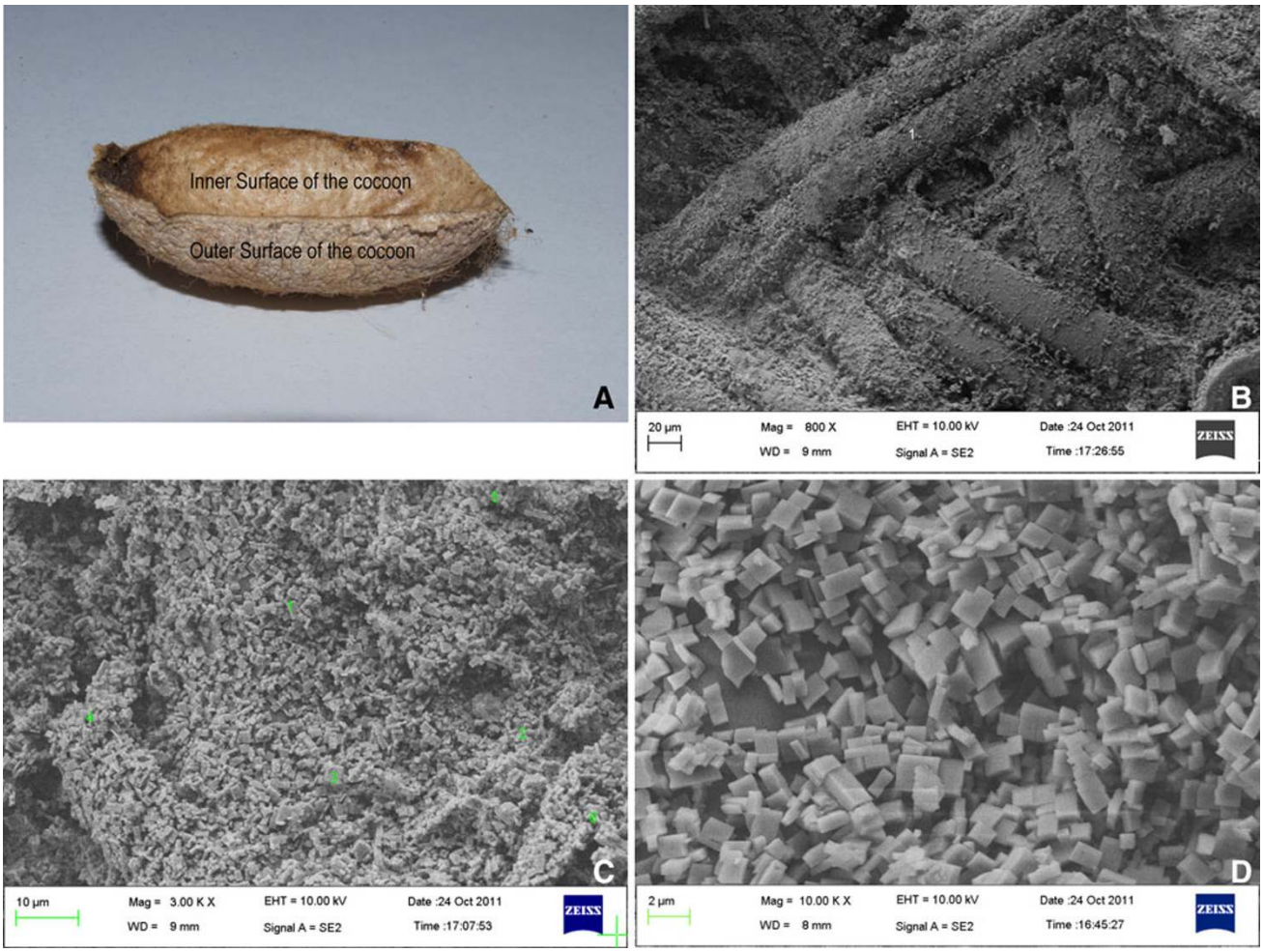

Fig. 3 **a** One half of the cocoon (*horizontal cut*, average length 5.0 cm) showing the inner (smooth) and the outer (coarse) surface morphology. **b** SEM image: the outer surface of the cocoon exhibiting the rough morphology. The particulate covering the surface of the silk fibers. **c** A high resolution SEM image of the outer surface of the cocoon showing the uneven texture due to the presence of crystals of different sizes. **d** At higher resolution SEM image cuboidal shaped crystals were irregularly stacked over one another. Dimension of the cuboidal crystals: the crystals were of approximately 1–2 µ in length and 1–2 µ in breadth. **e** The SEM image of the inner surface of the cocoon exhibits a smooth texture with intertwined silk fibers crisscross' the surface. **f** It shows the inner surface between the fibers with irregular gaps with few particulates. There were very few crystals found in the inner surface of the cocoon. **g** SEM image of the outer surface of the cocoon after the calcium oxalate monohydrate layer has been leached out. The outer surface of the cocoon showing smooth texture after removal of the calcium oxalate monohydrate crystals. **h** Outer surface of the treated cocoon at a high resolution SEM image showing the spots where calcium oxalate monohydrate crystals were embedded in the native cocoon prior to leaching. **i** SEM image of the inner surface of the cocoon after leaching away of the calcium oxalate monohydrate from the outer surface. As noticed earlier in the untreated cocoon, the SEM image of the inner surface of the cocoon exhibits a smooth texture with intertwined silk fibers criss-crossing the surface

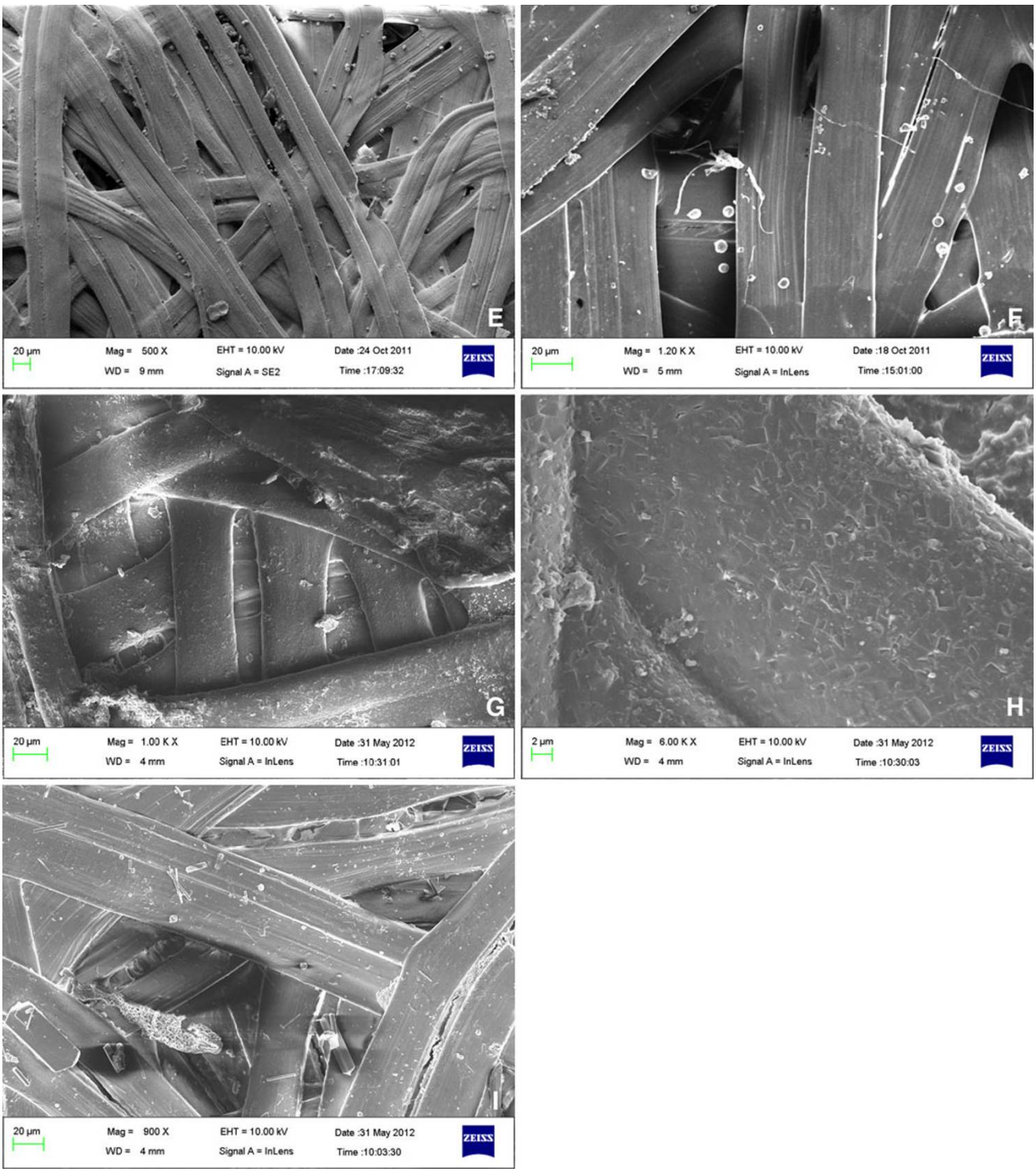

Fig. 3 continued

is filtered, washed with cold water and dried under ambient condition and subjected to XRD analysis. There is no doubt about the identity of this white precipitate as calcium oxalate monohydrate whose diffraction pattern is super imposable with the XRD pattern of pure calcium oxalate monohydrate and also with the calcium oxalate scrapped out from the untreated cocoon. Based on this result, we concluded that calcium oxalate monohydrate crystals are distributed differentially on the outer and the inner surfaces of the cocoon.

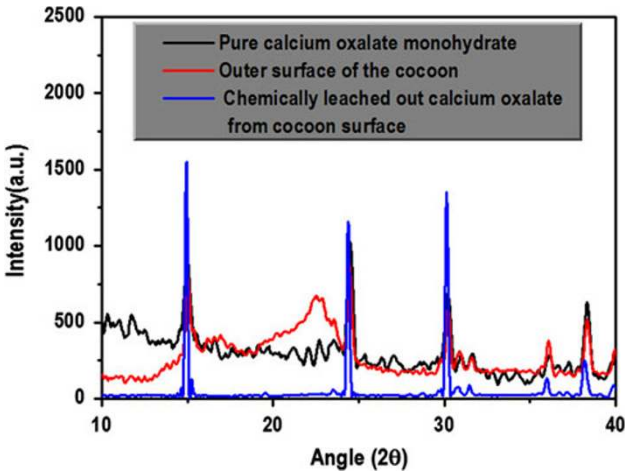

Fig. 4 Super imposed XRD pattern of pure calcium oxalate monohydrate, calcium oxalate monohydrate scrapped out from the untreated cocoon and calcium oxalate recovered from the leached out solution obtained from the outer surface of the cocoon

3.5 FTIR Analysis

We further validated the presence of calcium oxalate monohydrate crystals on the outer surface of the cocoon using FTIR spectroscopy (Fig. 5a–c). FTIR spectrum of pure calcium oxalate monohydrate is shown in Fig. 5a. FTIR spectrum of the outer surface of the cocoon is shown in Fig. 5b. FTIR spectrum of chemically leached calcium oxalate from outer surface of cocoon is shown in Fig. 5c. The very strong vibration at 1,632 cm^{-1} is assigned to asymmetric v_a(CO) vibration and the strong vibration at 1,316 cm^{-1} is assigned as symmetric v_s(CO) vibration of the oxalate group. The other low energy vibrations are related to mixed vibrations arising from stretching and bending mode including water in the lattice and ring deformation. Similarly the higher wave number broad absorption around 3,447 cm^{-1} as observed from the raw outer surface of the cocoon shows the presence of other functional groups in addition to the vibration arising out of v(OH) due to the presence of water. The weak vibrations lower than 3,000 cm^{-1} in raw cocoon strongly suggest the presence of some v(CH) and the background absorption in the 1,600–1,000 cm^{-1} region supports the presence of other vibrations related to silk residue. This is plausible as scrapping of the calcium oxalates from the surface may result a part of silk along with it. Such vibrations are absent in the chemically leached out calcium oxalate and also from pure calcium oxalate as seen in their respective IR spectrum where the dominant peaks related to the vibration of oxalate appeared. Thus FTIR spectroscopy supports the presence of calcium oxalate hydrate on the outer surface of the cocoons which is confirmed by XRD study [22].

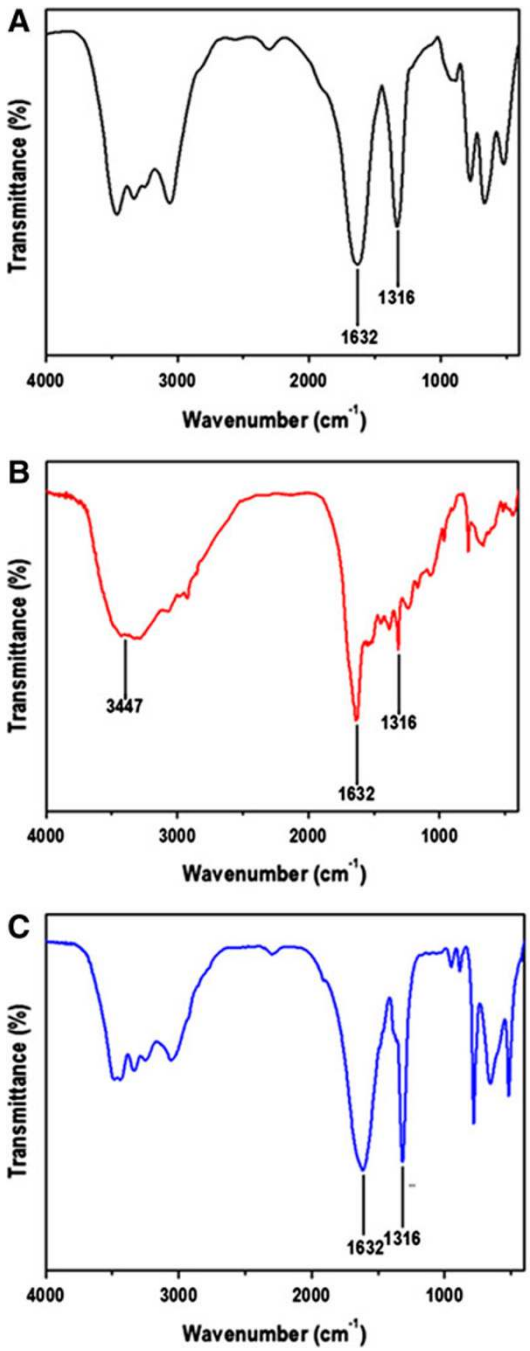

Fig. 5 **a** FTIR spectra of pure calcium oxalate monohydrate. **b** FTIR spectra of calcium oxalate monohydrate scrapped out from the untreated cocoon. **c** FTIR spectra of the calcium oxalate monohydrate recovered from the leached out solution obtained from the outer surface of the cocoon

3.6 EDAX Analysis

The EDAX analysis of the outer and the inner surface of the cocoon membrane shows the presence of 24 different elements (Fig. 6). These elements are distributed unequally on the outer and the inner surface of the cocoon membrane.

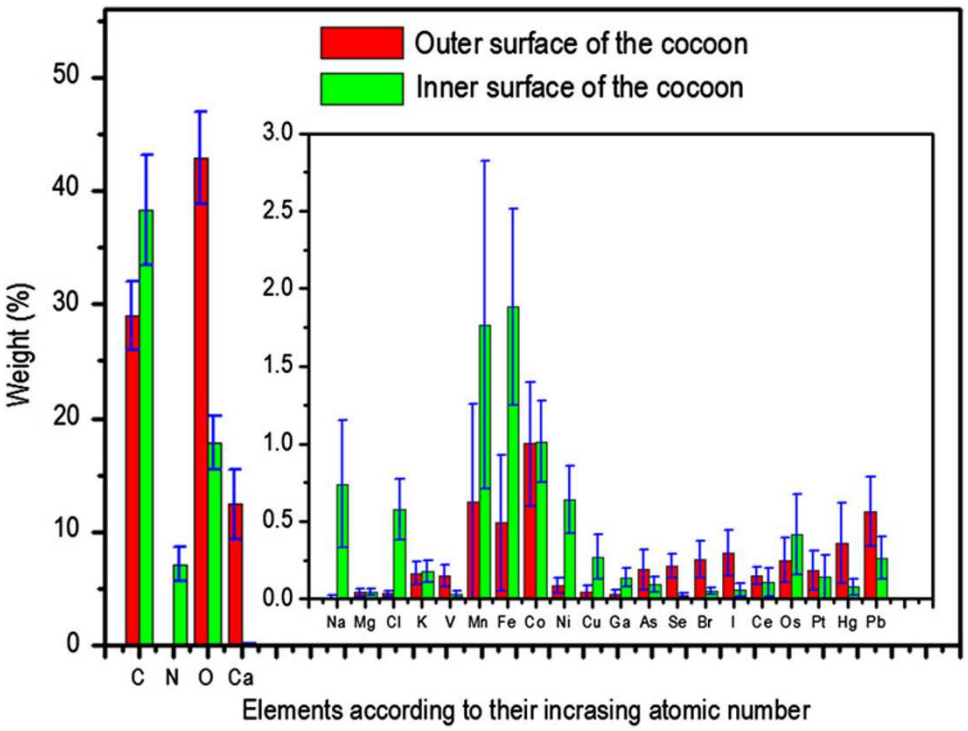

Fig. 6 Weight percentage values of the different elements present on the outer and the inner surfaces of the cocoon which were analyzed using EDAX. Data were collected for each element after analyzing the inner and outer surfaces of 6 different cocoons (n = 6)

Figure 6 shows the presence of 4 major elements (C, N, O and Ca) and 20 trace elements (Na, Mg, Cl, K, V, Mn, Fe, Co, Ni, Cu, Ga, As, Se, Br, I, Ce, Os, Pt, Hg, Pb) in varying concentrations on both the outer and inner surfaces of the cocoon. Data were collected for each element after analyzing the inner and outer surfaces of 6 different cocoons (n = 6). Significantly higher (at p = 0.01) weight percentage of Ca was observed on the outer surface (12.41 ± 3.05, n = 6) as compared to the inner surface (0.12 ± 0.05, n = 6). Similarly O was significantly higher (at p = 0.001) on the outer surface (42.88 ± 4.06, n = 6) as compared to the inner surface (17.84 ± 2.33, n = 6). On the contrary, N was found to be significantly low (at p = 0.001) on the outer surface as compared to the inner surface (7.15 ± 1.53, n = 6). Ca is significantly higher on the outer surface which is due to the presence of calcium oxalate monohydrate crystals on the outer surface. The significant presence of N on the inner surface may represent the fibrous silk proteins. The weight percentages of Na, Cl and Ni were significantly high (at p = 0.05) on the inner surface whereas Se was present at significantly higher (at p = 0.05) concentration on the outer surface. All the other elements did exhibit certain trend but were not found to be statistically significant. Presence of some of these elements on cocoon surface was previously reported in other studies [9, 23]

3.7 Asymmetric Nature of the Cocoon Membrane

Based on the SEM, EDAX, XRD and FTIR analysis, we concluded that the cocoon membrane is asymmetric. The asymmetric properties of the cocoon membrane are attributed to the significantly different distribution of calcium oxalate, nitrogen, sodium, nickel and selenium on the outer and the inner surfaces of the cocoon membrane. One of the earlier report, indicated the presence of crystals on the surface of the cocoon [24]. Thereafter those crystals are identified as calcium oxalate monohydrate by X-ray diffraction (XRD) studies [15, 25]. Another study further demonstrated that these crystals are formed in the larval gut [26]. Although these studies demonstrated the presence of calcium oxalate crystals on the cocoon surface but we are reporting for the first time that calcium oxalate is asymmetrically distributed on the outer and the inner surfaces of the cocoon membrane. Apart form it, this is the first evidence showing the differential distribution of nitrogen, sodium, chloride, nickel and selenium on the outer and the inner surfaces of the cocoon membrane. We believe that presence of these plethora of elements in the cocoon membrane is directly correlated with the kind of vegetation on which the larva is feeding.

3.8 CO_2 Flow Across the Native Cocoon Membrane

Based on the observed asymmetric property of the membrane, we hypothesize that it may be responsible in maintaining an ambient atmosphere inside the cocoon. Cocoon is a close structure. If excess CO_2 gets trapped inside such a close structure, then this will lead to a greenhouse like effect. Such a situation could be detrimental for the development of the pupa. To ensure an ambient

environment inside the cocoon, it should be equipped with an efficient mechanism to get rid-off the CO_2 generated inside. To test this hypothesis, we measured the minimum time taken by CO_2 to diffuse out of the cocoon when CO_2 was injected inside the cocoon (Fig. 2a). The minimum mean time for CO_2 to diffuse out of the cocoon was 20.18 ± 4.32 s, $n = 11$ (mean $\pm$ standard error, n = number of cocoons). When we measured the diffusion of CO_2 inside the cocoon from outside for 10 min, no appreciable concentration of CO_2 was found inside ($n = 11$) (Fig. 2b). These two experiments demonstrate CO_2 gating which regulates unidirectional flow of CO_2 across the silk cocoon membrane.

3.9 CO_2 Flow Across the Cocoon Membrane in Which Calcium Oxalate Layer from the Outer Surface is Removed

Calcium oxalate free cocoons were used to study the CO_2 flow across the cocoon membrane. The minimum mean time for CO_2 to diffuse out of the cocoon was 17.83 ± 1.27 s, $n = 6$ (mean $\pm$ standard error, n = number of cocoons). The minimum mean time for CO_2 to diffuse inside the cocoon from outside CO_2 rich environment was 118.33 ± 43.54 s, $n = 6$ (mean $\pm$ standard error, n = number of cocoons)

3.10 O_2 Flow Across the Cocoon Membrane

To understand the diffusion of O_2 across the membrane, we performed similar experiment under O_2 atmosphere. The experimental set-up to monitor the passage of O_2 across the cocoon membrane is described in Fig. 2c, d. The average minimum time needed for O_2 to diffuse out of the cocoon was 33.16 ± 9.05 s, $n = 6$ (mean $\pm$ standard error, n = number of cocoons). The average minimum time needed for O_2 to diffuse inside the cocoon from outside was 34.50 ± 6.07 s, $n = 6$ (mean $\pm$ standard error, n = number of cocoons). These indicate that the rate of O_2 diffusion across the cocoon membrane remains the same.

3.11 CO_2 Gating (Unidirectional Flow of CO_2) and Bidirectional Flow of O_2

To the best of our knowledge, this is the first evidence showing the unidirectional flow of CO_2 across the cocoon membrane. We have found that in native cocoon the CO_2 flows from inside to outside the cocoon and the reverse flow is prevented. We propose that such a CO_2 gating helps in maintaining an ambient gaseous environment inside the cocoon. We observed a bidirectional flow of O_2 across the cocoon membrane. There is also a recent report on the bidirectional diffusion of O_2 across the cocoon membrane [19]. Whether the asymmetric structural features of the cocoon membrane is responsible for the unidirectional flow of CO_2 requires some explanation. In order to establish a structure–function activity of the asymmetric cocoon membrane, we devised a strategy to remove the major component from the outer surface of the cocoon, namely calcium oxalate monohydrate, which is believed to impart asymmetry in the structure. The calcium oxalate monohydrate free cocoon when subjected to CO_2 diffusion experiment shows some interesting results which are tabulated above. A comparison of this data with the untreated cocoon show the permeability of CO_2 from inside to outside the cocoon has increased slightly with a mean value of 17 s compared to the mean value of 20 s in the untreated cocoon. However, for the reverse passage that is from outside to inside, the treated cocoon could not withstand a longer time of 10 min what was observed with the untreated cocoon and the CO_2 could be sensed only after 2 min. Such experiment directly relates the important role of heterogeneity of cocoon shell with the deposition of calcium oxalate hydrate crystals. Our results show that without the presence of calcium oxalate monohydrate, a delay of CO_2 passage from outside to inside could be directly related to the weaving of silk thread. This is important in the sense that there are different version of cocoons where the deposition of calcium oxalate hydrate type of crystals on the outer surface varies [15, 18]. Therefore it is the calcium oxalate crystals which predominantly prevents the passage of CO_2 from outside to inside. Yet the weaving pattern of silk in the membrane also contributes to the gating of CO_2. It is true that the environmental partial pressure of CO_2 (0.228 mm of mercury) is much less than what we had used in our experiment which is significantly much higher in concentration because to reduce time in its passage for ready identification [27]. Therefore the flow of CO_2 from outside to the inside of the cocoon could be negligible with the real concentration of CO_2 available in the environment (atmosphere contains 0.03 % of CO_2). The dependency of CO_2 flow with the varied concentration of CO_2 versus time is under study based on untreated and treated cocoon. However qualitatively it is clear to report that the intrinsic weaving pattern of silk does contribute to the gating of CO_2 which is supplemented by the deposition of calcium oxalate crystals on the outer surface of the cocoon.

3.12 Possible Role of Calcium Oxalate Monohydrate Layer in CO_2 Gating

The role of calcium oxalate monohydrate to prevent the flow of CO_2 from outside to inside needed a chemical explanation. It is known that calcium oxalate hydrate prefers a humid environment and under humid condition the

CO_2 from the atmosphere gets hydrated to form carbonic acid. The carbonic acid can be dissociated to bicarbonate and proton and the outer surface of the cocoons predominantly with calcium oxalate monohydrate may influence this dissociation forming some hydrogen bonded network. The strong electronegative oxygen atoms of oxalate groups readily assist in creating such hydrogen bonded network. The external CO_2 thus lost its small entity and may be trapped by such hydrogen bonding network. The outcome of such phenomenon is the prevention of the free passage of CO_2 from outside to the inside of the surface of the cocoon. In fact the role of the calcium oxalate hydrate thus can be thought as the material which continuously blocked CO_2 on the surface. Any leakage of CO_2 from the outer surface faces the second barrier by the weaving pattern of silk which behaves as the final filter inside. This explanation is based on the existing knowledge of chemistry of hydrogen bonding of CO_2. Our present work clearly proves the gating of CO_2 across the cocoons. In future, if we could mimic such a membrane then it could be used as a gas filter and for developing green energy saving housing material.

3.13 Thermoregulation

On the aspect of thermoregulation inside the cocoon, we performed experiments simulating the weather conditions that a cocoon can experience by varying the temperature ranging from 5 to 50 °C with relative humidity (RH) varying from 30 to 80 %. After placing a cocoon, in an incubator maintaining such temperature and humidity conditions and allowing an hour to attain equilibrium, the inside temperature of the cocoon is noted. On exposure of 5 °C temperature, the inside temperature of the cocoon became stable at 25.01 ± 0.18 °C, n = 8 (mean ± standard error, n = number of cocoons) after 1 h. Similarly with an outside temp of 50 °C, the inside temp is stabilized at 34.71 ± 0.81 °C, n = 8 (mean ± standard error, n = number of cocoons) after an hour. Thus cocoon membrane has an intrinsic temperature controlling system to offer a physiological temperature regime inside the cocoon. A thermoregulatory mechanism in hornet silk, hornet's nest, and in the cocoon of *Bombyx mori* was proposed earlier [9, 20, 21, 28]. Our results are supporting the earlier finding.

4 Conclusions

In this paper, we show the architectural marvel displayed by the silkworm during its metamorphosis. The cocoon it builds from its own secretion is so designed to house it for weeks to months till it transformed to a full grown adult moth. During this transformation period from larvae to pupa the cocoon controls gas flow and thermal regulation for its survival inside. The knowledge gained by such architectural sophistication albeit with simple resources will focus us to go for the development of environment friendly, energy saving building materials and gas filters.

Acknowledgments The work was supported by IITK start-up Grant (IITK/BSBE/20100206) of MD. MR is a senior research fellow of CSIR, India (Fellowship Number: 09/092(0670)/2009-EMR-I) and this work is part of his doctoral thesis. TK is funded by IIT Kanpur doctoral fellowship. Authors are thankful to DST unit on Nanosciences at IIT Kanpur for providing XRD facility. Authors are thankful to the two anonymous reviewers who suggestions enormously helped in improving the quality of the work.

References

1. Trouvelot L (1867) Am Nat 1(2):85–94
2. Packard AS (1898) A text book of entomology. The Macmillan Company, New York
3. Johnson SA (1989) Silkworms. First Avenue Editions, Minneapolis
4. Voigt WH (1965) Z Zellforsch Mikrosk Anat 66(4):571–582
5. Voigt WH (1965) Z Zellforsch Mikrosk Anat 66(4):548–570
6. Prudhomme JC, Couble P (1979) Biochimie 61(2):215–227
7. Vollrath F (1992) Sci Am 266:70–76
8. Vollrath F (1999) Int J Biol Macromol 24(2–3):81–88
9. Kirshboim S, Ishay JS (2000) Comp Biochem Physiol A Mol Integr Physiol 127(1):1–20
10. Shao Z, Vollrath F (2002) Nature 418(6899):741
11. Joseph Z, Ishay JS (2004) J Electron Microsc (Tokyo) 53(3):293–304
12. Yonemura N, Sehnal FJ (2006) Mol Evol 63(1):42–53
13. Chen F, Porter D, Vollrath F (2010) Phys Rev E Stat Nonlin Soft Matter Phys 82(4 Pt 1):041911
14. Pandiarajan J, Cathrin BP, Pratheep T, Krishnan M (2011) Rapid Commun Mass Spectrom 25(21):3203–3206
15. Teshome A, Vollrath F, Raina SK, Kabaru JM, Onyari J (2012) Int J Biol Macromol 50(1):63–68
16. Kundu SC, Kundu B, Talukdar S, Bano S, Nayak S, Kundu J, Mandal BB, Bhardwaj N, Botlagunta M, Dash BC, Acharya C, Ghosh AK (2012) Biopolymers 97(6):455–467
17. Chen F, Porter D, Vollrath F (2012) J R Soc Interface. doi: 10.1098/rsif.2011.0887
18. Chen F, Porter D, Vollrath F (2012) Acta Biomater 8(7):2620–2627
19. Blossman-Myer B, Burggren WW (2010) Comp Biochem Physiol A Mol Integr Physiol 155(2):5
20. Ishay JS, Barenholz-Paniry V (1995) J Insect Physiol 41(9):7
21. Huang X, Liu G, Wang X (2012) Adv Mater 24(11):1482–1486
22. Nakamoto K (1986) Infrared and Raman Spectra of inorganic and coordinated compounds, 4th edn. Wiley, New York
23. Wilaiwan S, Chirapha B, Yaowalak S, Prasong S (2010) J Appl Sci 10:575–579
24. Dewitz J (1921) Zoologische Jahrbucher Abteilung fuer Allgemeine Zoologie und Physiologie der Tiere 38:365–404

25. Ohnishi E, Takahashi SY, Sonobe H, Hayashi T (1968) Science 160(3829):2
26. Teigler DJ, Arnott HJ (1972) Nature 235(5334):166–167
27. Vogel AI (1961) A text book of quantitative inorganic analysis, 3rd edn. Longmans, London
28. Danks HV (2004) Eur J Entomol 101:433–437